

Molecular Pharmacology

P6981 inhibits DNA binding of B-ZIP protein at low nM concentrations

P6981, an arylstibonic acid, is a novel low nanomolar inhibitor of CREB binding to DNA

Jianfei Zhao, Jason R. Stagno, Lyuba Varticovski, Eric Nimako, Vikas Rishi, Kathy McKinnon, Rhone Akee, Robert H. Shoemaker, Xinhua Ji, and Charles Vinson

Laboratory of Metabolism (J.Z., E.N., V.R., C.V.), National Cancer Institute, Bethesda, MD 20892; Macromolecular Crystallography Laboratory (J.S., X.J.), National Cancer Institute, Frederick, MD 21702; Laboratory of Receptor Biology and Gene Expression (L.V., K.M.), Vaccine Branch, National Cancer Institute, Bethesda, MD 20892; Natural Products Support Group (R.A.), SAIC-Frederick, Frederick, MD 21702; and Developmental Therapeutics Program (R.H.S.), Frederick National Laboratory for Cancer Research, Frederick, MD 21702

Table of Contents

Supplemental Figure Legends	S2
Supplemental Table 1	S3
Supplemental Table 2	S3
Supplemental Table 3	S4
Supplemental Table 4	S4
Supplemental Materials and Methods	S5
Supplemental References	S5
Supplemental Fig. 1	S6
Supplemental Fig. 2	S7
Supplemental Fig. 3	S8
Supplemental Fig. 4	S9
Supplemental Fig. 5	S10

Molecular Pharmacology
P6981 inhibits DNA binding of B-ZIP protein at low nM concentrations

Supplemental Figure Legends

Supplemental Fig. 1. Purity of P6981 (*A*) and NSC13746 (*B*). The top chromatogram is from the evaporative light scattering detector (ELSD) and the lower trace is the photodiode array detector (PAD) at 264 nm. Purity was determined using the ELSD.

Supplemental Fig. 2. Thermal denaturations of VBP and CREB LZ domains with or without P6981. *A*, Thermal denaturation of 2 μ M commercially synthesized 47-amino-acid VBP LZ dimer (VBP47) or 2 μ M CREB LZ dimer (CREB-LZ) in the absence or presence of P6981. No P6981 (○), 50 μ M P6981 (●). *B*, Sequence alignment of CREB-LZ, VBP-LZ (used in Fig. 4*B*), VBP47, and VBP39 (used in Fig. 5). ASMTGGQQMGRDP is the ϕ 10 tag.

Supplemental Fig. 3. Salt effects on the interactions of P6981 and VBP B-ZIP domain. The thermal denaturation of 2 μ M VBP B-ZIP domain dimer with or without 50 μ M P6981 in the buffer used in the main figures with varying KCl concentrations: 15 mM (*A*), 150 mM (*B*), 2,000 mM (*C*) KCl.

Supplemental Fig. 4. The genotype of the clear cell sarcoma cell line. PCR of genomic DNA from clear cell sarcoma and K562 cells identified a specific fragment (denoted by an arrow) with EWS-ATF1 type 2 primer sets, but not with any other primer sets corresponding to known genotypes of clear cell sarcoma (Panagopoulos et al., 2002).

Supplemental Fig. 5. Representative flow cytometry data used in Fig. 9*A* and *B* showing P6981 induced CCS-1 growth arrest. CCS-1 cells were either untreated (left panels) or treated with 25 μ M P6981 (middle panels) or NSC13778 (right panels). Each sample was analyzed in biological replicates.

Molecular Pharmacology
P6981 inhibits DNA binding of B-ZIP protein at low nM concentrations

Supplemental Table 1

IC₅₀ values of 25 arylstibonic acids for five B-ZIP or B-HLH-ZIP transcription factors.

Active arylstibonic acid compounds are ranked according to their inhibitory potencies to the five tested proteins. IC₅₀ values were estimated by EMSA shown in Fig. 2 and 4.

Compound	IC ₅₀ (μM)				
	CREB	C/EBPα	VBP	Mitf	USF
P6981	0.005*	0.02*	<0.1	0.6	0.2
P6982	<0.1	0.09	0.2	0.6	0.2
NSC13778	<0.1	0.2	0.2	0.6	0.2
NSC13746	0.06*	0.05*	0.5	0.6	0.6
NSC13759	0.1	0.1	0.6	0.6	0.6
NSC13760	0.6	0.6	0.6	0.6	0.6
P7795	<0.1	0.1	1.9	6.5	6.5
P6987	0.2	0.09	0.5	0.6	0.2
P7796	<0.1	0.3	0.7	6.5	6.5
P6971	0.3	0.6	0.6	0.9	0.8
P6970	0.9	1.0	0.8	1.0	0.9
P6966	0.2	0.6	0.6	2.2	0.5
P6954	0.3	0.6	0.6	6.5	0.9
NSC732942	0.2	0.6	0.5	6.0	6.5
NSC13755	0.8	2.0	1.0	5.3	1.0
NSC15578	1.1	0.6	1.0	6.5	6.5
P6953	0.5	2.0	2.5	5.0	6.4
NSC13793	1.0	2.0	1.0	6.2	10.0
P7794	0.2	0.1	>10.0	>10.0	10.0
P6964	6.5	2.0	6.5	>10.0	6.5
P6968	2.7	6.5	0.8	>10.0	>10.0
NSC13782	3.2	1.9	>10.0	10.0	>10.0
NSC13765	7.0	2.0	6.5	6.5	6.5
NSC732943	6.5	2.0	5.4	>10.0	6.5
NSC13771	>10.0	2.0	>10.0	>10.0	>10.0

* See Fig. 4 for details.

Supplemental Table 2

Effect of KCl and P6981 concentrations on the melting temperatures (T_m) of VBP B-ZIP and LZ (leucine zipper). T_ms were determined using data from supplemental Fig. 3.

Protein	[P6981] (μM)	[KCl] (mM)	T _m (°C)		
			15	150	2,000
VBP B-ZIP	0		50.1	50.0	57.6
	50		57.2	53.6	56.4
VBP LZ	0		57.7	56.0	57.2
	50		60.4	57.0	58.6

Molecular Pharmacology
P6981 inhibits DNA binding of B-ZIP protein at low nM concentrations

Supplemental Table 3

X-ray diffraction data and refinement statistics.

Crystal	VBP39-NSC13778
Space group	<i>P</i> 6 ₁
Unit cell parameters	
<i>a</i> , <i>b</i> (Å)	68.8
<i>c</i> (Å)	77.2
Matthews coefficient (Å ³ /Da)	3.9
Data	Overall / (Last shell)
Resolution (Å)	34.42-3.30 (3.39-3.30)
Unique reflections	3,054 (238)
Redundancy	4.0 (3.9)
Completeness (%)	96.3 (92.6)
<i>R</i> _{merge} ^a	0.115 (0.495)
<i>I</i> / σ (<i>I</i>)	14.9 (3.5)
Refinement	Overall / (last shell)
Resolution (Å)	34.42-3.30 (4.16-3.30)
Unique reflections	3,042 (1,505)
Completeness (%)	96.0 (96.0)
Data in the test set	254 (122)
<i>R</i> _{work}	0.258 (0.315)
<i>R</i> _{free}	0.278 (0.282)
Structure	
Protein non-H atoms / B (Å ²)	594 / 54.3
NSC13778 non-H atoms / B (Å ²) ^b	15 / 142.0
Solvent atoms / B (Å ²)	5 / 13.7
R.m.s.d.	
Bond lengths (Å)	0.013
Bond angles (°)	1.621
Ramachandran plot	
Favored regions (%)	97.14
Outliers (%)	2.86

^a $R_{\text{merge}} = \sum |(I - \langle I \rangle)| / \sum (I)$, where *I* is the observed intensity.

^b Sb atom refined anisotropically.

Supplemental Table 4

Weight of mice xenografted with CCS-1.

	NSC13778 Treated					P value
Day 0	19.2	22.4	24.5	24	30.3	
Day 37	20.1	19.4	22.4	24	31.8	0.57
Vehicle Control						
Day 0	27.6	26.9	28.2	31.4	29.8	29.9
Day 37	28.6	29.2	26.1	26.3	23.5	0.13

Molecular Pharmacology

P6981 inhibits DNA binding of B-ZIP protein at low nM concentrations

Supplemental Materials and Methods

Genotyping—PCR was conducted using REDExtract-N-Amp Tissue PCR Kits (Sigma-Aldrich). Cell lysates were extracted from the EWS-ATF1 clear cell sarcoma and K562 cells according to the manufacturer's instructions. The thermal cycling of PCR is: initial denaturation at 95 °C for 5 min, 34 cycles (94 °C for 1 min, 62 °C for 30 sec, and 72 °C for 30 sec), followed by 10 min at 72 °C. Primers are as the following (5' to 3'; (Wang et al., 2009)):

EWS-ATF1 type 1

Forward: ATCGTGGAGGCATGAGCAGA

Reverse: TCTGGAGTTCTGCTGCTGTCA

EWS-ATF1 type 2

Forward: TAGTTACCCACCCCAAATGGAA

Reverse: CCATCTGTGCCTGGACTTGC

EWS-ATF1 type 3

Forward: ATCGTGGAGGCATGAGCAGA

Reverse: CCATCTGTGCCTGGACTTGC

EWS-ATF1 type 4

Forward: TAGTTACCCACCCCAAATGGAA

Reverse: CTCGGTTTCCAGGCATTTCAC

EWS-CREB1 type 1 (CREB and ATF1)

Forward: TCCTACAGCCAAGCTCCAAGTC

Reverse: TCCATCAGTGGTCTGTGCATACTG

EWS-ATF1 type 2 (CREB specific)

Forward: TCCTACAGCCAAGCTCCAAGTC

Reverse: GTACCCCCATCGGTACCATTGT

Analytical HPLC—The evaporative light scattering detector and Photodiode Array Detector were used to analyze the purity of P6981 and NSC13746. The analytical HPLC system consisted of the following instruments: Waters 600 Gradient Pump, Waters 2767 Sample Manager, Waters Micromass ZQ Mass Spectrometer, operating in Electrospray Ionization (ESI) mode, Waters 2998 Photodiode Array detector, and Sedere Sedex 75 Evaporative Light Scattering detector. The Micromass Masslynx 4.1 data acquisition software package was used to acquire and process chromatographic data (Simmons and McCloud, 2003). The analytical HPLC column was a Hamilton PRP-X100 Anion Exchange (column Size: 4.6 mm (i.d.) x 250 mm (L)). The following solvent systems were used as the eluent:

Flow Rate: 1.5 ml/min. Bottle A: 50 mM aq. ammonium acetate, pH 9.0. Bottle B: 200 mM aq. ammonium acetate, pH 9.0. Gradient Elution: At 0-5min, 0% B; 5-20 min, linear gradient from 0% B to 100% B; 20 min to end, 100% B. The evaporative light scattering detector was essential for determining the purity of these arylstibonic acids since the reagents used to synthesize the arylstibonic acids and the impurities or side-products do not have a UV chromophore.

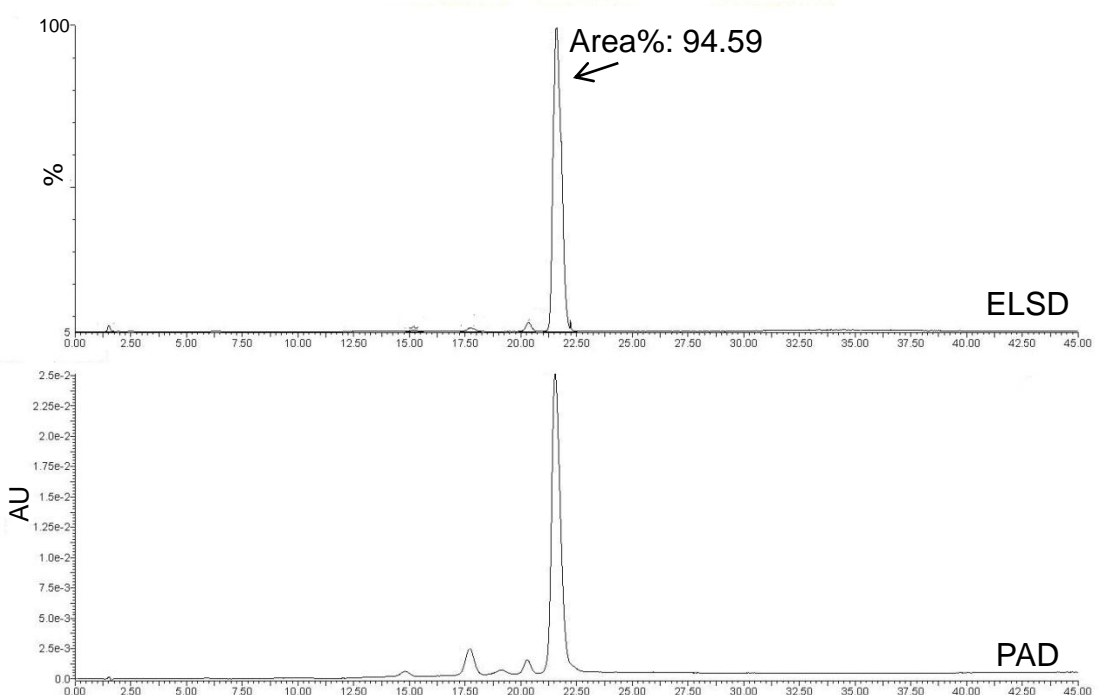
Supplemental References

- Panagopoulos I, Mertens F, Debiec-Rychter M, Isaksson M, Limon J, Kardas I, Domanski HA, Sciot R, Perek D, Crnalic S, Larsson O and Mandahl N (2002) Molecular genetic characterization of the EWS/ATF1 fusion gene in clear cell sarcoma of tendons and aponeuroses. *Int J Cancer* **99**(4):560-567.
- Simmons TL and McCloud TG (2003) Analysis of stibonic acids by ion exchange chromatography with ESI-MS/photodiode array detection. *J Liq Chromatogr R T* **26**(13):2041-2051.
- Wang WL, Mayordomo E, Zhang WY, Hernandez VS, Tuvin D, Garcia L, Lev DC, Lazar AJF and Lopez-Terrada D (2009) Detection and characterization of EWSR1/ATF1 and EWSR1/CREB1 chimeric transcripts in clear cell sarcoma (melanoma of soft parts). *Modern Pathol* **22**(9):1201-1209.

Supplemental Fig. 1

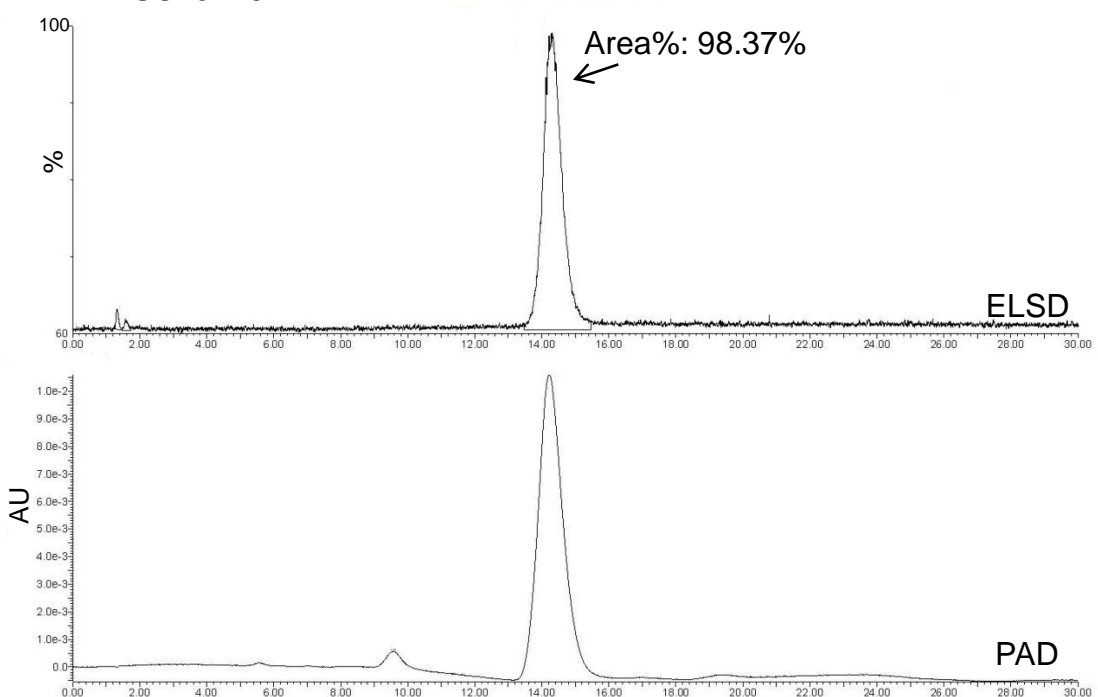
A

P6981

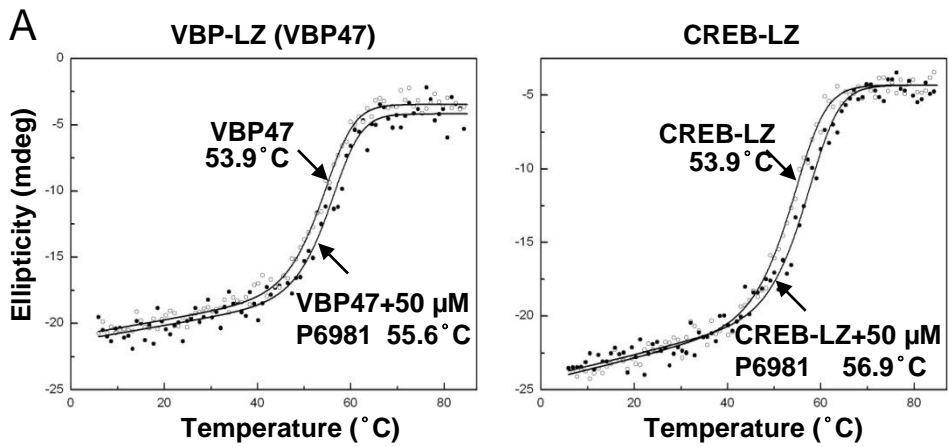


B

NSC13746



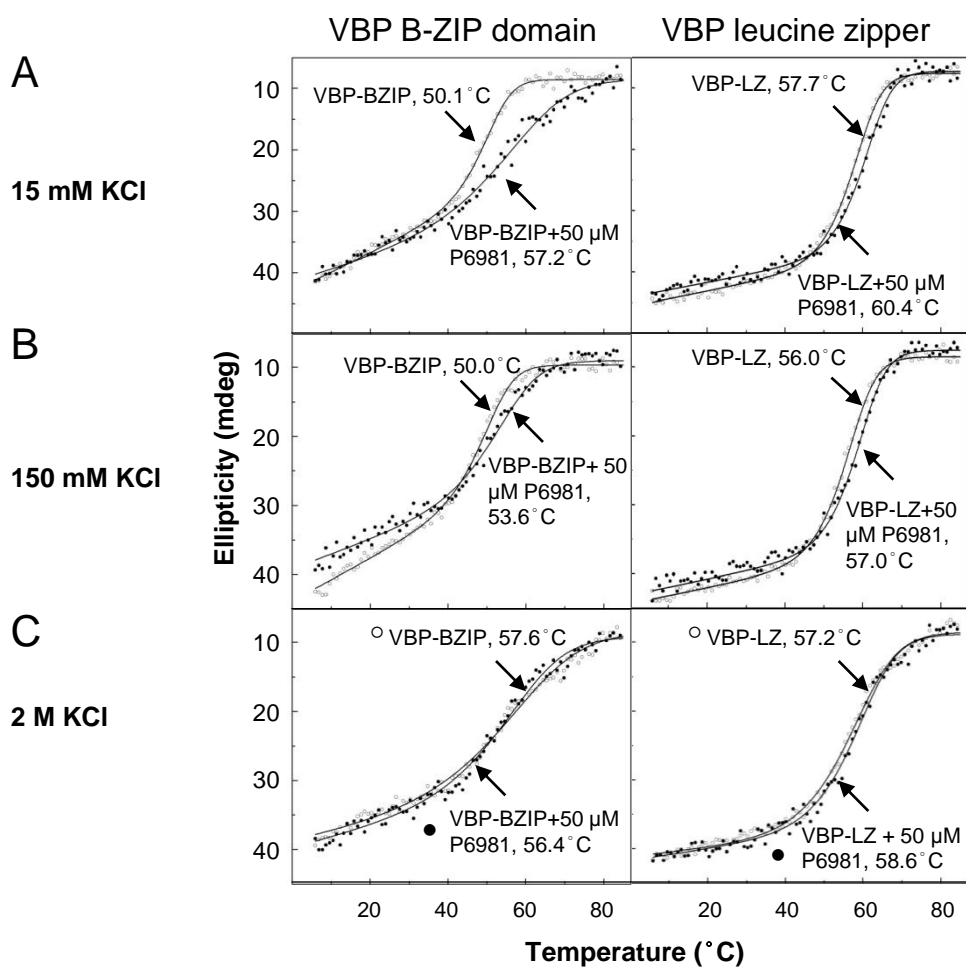
Supplemental Fig. 2



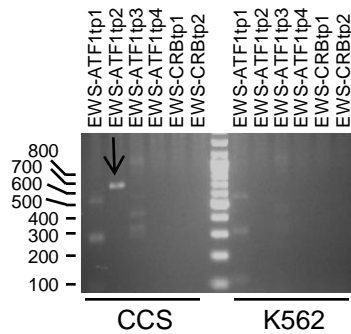
B

CREB-LZ	ASMTGGQQMGRDP LEN RVAVLEN QNKTLIE ELKALKD LYCHKSD
VBP-LZ	ASMTGGQQMGRDP ITI RAAFLEK ENTALRT EVAELRK EVGRCKN IVSKYET RYGPL
VBP-LZ (VBP47)	RDPD LEI RAAFLEK ENTALRT EVAELRK EVGRCKN IVSKYET RYGPL
VBP-LZ (VBP39)	RDPD LEI RAAFLEK ENTALRT EVAELRK EVGRCKN IVSK
	gabcdef gabcdef gabcdef gabcdef gabcdef
	L_0 L_1 L_2 L_3 L_4 L_5

Supplemental Fig. 3

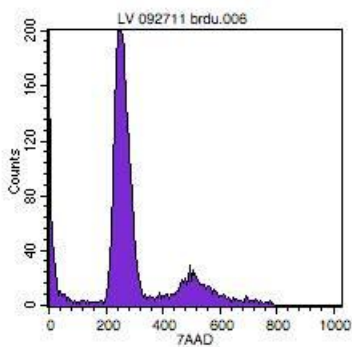


Supplemental Fig. 4

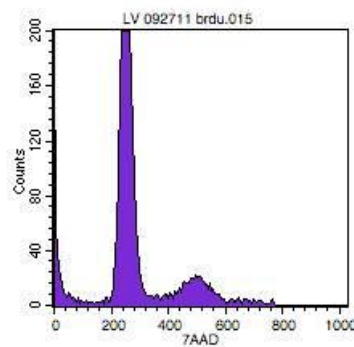


Supplemental Fig. 5

Untreated



25 μ M P6981



25 μ M NSC13778

